

Instabilities in a running superfluid: boosted superfluid and stripe supersolid

Jinwu Ye

¹ Institute for Theoretical Sciences, Westlake University, Hangzhou, 310024, Zhejiang, China

² Department of Physics and Astronomy, Mississippi State University, MS, 39762, USA

(Dated: October 11, 2022)

The possible instabilities in a running superfluid has been a long-time historical problem since first studied by L. P. Landau. By constructing effective actions in terms of suitable order parameters, we revisit this outstanding open problem at $d = 2$ and $d = 3$. We find that if the instability is driven by the SF Goldstone mode near $k = 0$, then there is a quantum Lifshitz transition from the SF to a Boosted SF (BSF) with the dynamic exponent ($z_x = 3/2, z_y = 3$) subject to logarithmic corrections from a marginally irrelevant cubic derivative term at $d = 2$ (becomes irrelevant at $d = 3$). This case may happen to exciton superfluids in 2d bilayer quantum Hall systems or electron-hole bilayer systems, especially in 2d weakly interacting Bose gas in cold atom systems. If the instability is driven by the roton mode near a finite momentum $k = k_0$, then there is a SF to a stripe supersolid transition with the dynamic exponent $z = 1$ which is in the same universality class as the $z = 1$ boosted Mott-SF transition studied previously in a different context. This case may apply to 3d Helium 4 and also 3d cold atom BECs with long-range interactions where the rotons in the SF phase plays an important role. Driving a SF sufficiently fast may become an effective way to create a SS which is a long time sought novel state of matter.

1. Introduction: It is well known that many systems become a superfluid at sufficiently low temperatures¹. He4 or He3 is the oldest strongly interacting bosonic or fermionic systems which become a SF below $T_c \sim 2.17K$ and $T_c \sim 1mK$ respectively. Since the discovery of the laser-cooling techniques, the weakly interacting superfluid systems were created in bosonic² and fermionic³ charge neutral atoms at even lower temperature $\sim nK$. There are also some experimental evidences to suggest exciton superfluid of electrons and holes may have been realized in the 2d bilayer quantum Hall systems in a strong magnetic field at the total filling factor $\nu_T = 1^4$ or electron-hole bilayer at zero magnetic field with sufficiently long lifetime⁵. In a quantum magnet subject to a Zeeman field, the $U(1)_s$ spin rotation symmetry around the Zeeman field resembles the global $U(1)$ symmetry in the interacting bosons⁸, the magnon condensations leading to some magnetic ordered phases can be mapped to the boson condensations leading to the SF. Recently, this mapping was also found in quantum magnets with spin-orbital couplings (SOC) in a longitudinal Zeeman field⁹.

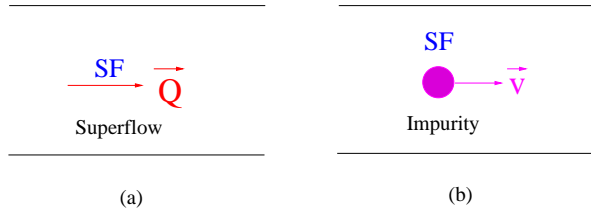


FIG. 1. (a) Driving a superfluid relative to a straight wall. It is also equivalent to moving the straight wall relative to the SF. (b) A moving impurity in a superfluid which is different than (a).

The physics of driving an object inside a superfluid (SF) or driving the SF itself has a long history¹¹⁻¹⁴. It may be necessary to distinguish the two different, but

related cases:

(1) Controlling the superfluid (Fig.1a): The SF is flowing with a finite velocity v with respect to a wide straight wall. It was also discussed in^{11,14} and more recently in¹⁶. The flow of a SF with $v > v_c^{SF}$ may not destroy SF, but the order parameter may develop small additional components around a roton minimum, therefore reduce the superfluid density. However, when increasing v further, the fate of SF is still not known yet. (2) Controlling the moving object (Fig.1b): An impurity moving in a superfluid. It was discussed in^{11,14} and more recently in¹⁵. If an object moves in a superfluid at $T = 0$ with a velocity below the critical velocity $v < v_c^O$, there is no viscosity. However, when $v > v_c^O$, a viscosity arises due to the emission of elementary excitations such as vortex rings^{12,13}. The two classes are completely different, so need separate discussions: the first class is an equilibrium steady one. The second one is a non-equilibrium driven system which was experimentally investigated in cold atom BEC, by pulling an optical lattice¹⁰. In this manuscript, we focus on the first class from effective action approach in either phase or dual density representation whichever is suitable. We will also establish some intrinsic connections between this class and a seemingly unrelated problem: the fate of liquid Helium under the increasing pressure investigated previously^{19,20,49}. While we relegate the discussions on the second class to the appendix B.

The global Pressure-Temperature (T-P) phase diagram¹⁴ of the Helium-4 is shown in Fig.2a. The elementary excitations in the Helium-4 consist of the SF phonon part near $k \sim 0$ and the roton part near $k = k_0$ (Fig.2b). In this well known T-P diagram, there maybe a room near the SF-Solid boundary to host a possible tantalizing supersolid phase which has both the off diagonal SF order and the diagonal solid order¹⁷. In 2005, by using a torsional oscillator measurement, Chan's

group¹⁸ observed a marked $1 \sim 2\%$ non-classical rotational inertial (NCRI) of the solid 4He at $\sim 0.2K$ when $P_c = 120\text{bar} < P < 170\text{bar}$, both when embedded in Vycor glass and in bulk Helium 4. The authors suggested that the NCRI may suggest the supersolid state of 4He . These experimental results inspired extensive theoretical^{19,20} and experimental interests to examine the very intriguing supersolid phase of 4He . However, a later refined experiment²¹ excludes the putative SS in Fig.2a. Despite its absence in the $\text{He}4$ system, the SS phase is an interesting phase on its own. It was shown to exist in a lattice system²²⁻²⁸. Of course, the SS in a lattice system is quite different than that in a continuum system²⁰. So a SS phase of matter in a continuum remains a science fiction.

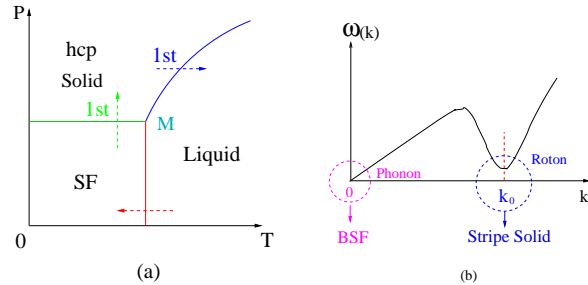


FIG. 2. (a) The pressure P and temperature T $\text{He}4$ phase diagram with $T_c \sim 2.13K$ and $P_c \sim 120\text{bar}$. The liquid to SF transition is in a classical 3d XY class for any pressure $0 < P < P_c$ which is also exactly marginal. The SF to solid transition is a first order quantum Lifshitz transition triggered by the lowering of roton surface tuned by the pressure⁴⁹. The liquid to solid transition is a first order classical Lifshitz transition driven by the peak in the density-density correlation tuned also by the pressure. A tantalizing possibility of a supersolid (SS) phase denoted by the dashed line turns out to be just a phase separation due to the 1st order SF to solid transition. (b) The elementary excitation in the SF phase. The roton surface is spherically symmetric with the roton gap $\Delta/k_B \sim 10K$ at the minimum $k_0 \sim 2\text{\AA}^{-1}$.

In this manuscript, we will show that the SS may also exist in Helium 4 under a sufficiently large drive, namely the second class of problem in the last paragraph. We develop an systematic and unified effective action approach in both the phase and its dual magnitude representation to study all the possible instabilities and quantum phase transitions (QPT) by driving a SF beyond some critical velocities. If the instability is due to the SF Goldstone mode near $k = 0$, then there is a quantum Lifshitz transition from the SF to a boosted SF (BSF) with the novel dynamic exponent ($z_x = 3/2, z_y = 3$) and a marginally irrelevant cubic derivative term at $d = 2$. We work out the excitation spectrum in both phases, perform the renormalization group analysis and evaluate the scaling functions at a finite T near the QPT. This scenario may also apply to the 2d exciton SF in BLQH⁴ and ELBL^{5,54} where the magneto-roton exists only at a very high energy, especially in cold atom BEC systems

which has very low critical velocities^{2,3}. If the instability is due to the roton mode near $k = k_0$, then there is a SF to a stripe supersolid (SSS) transition with the dynamic exponent $z = 1$ which is in the same universality class of the boosted Mott-SF transition studied in^{9,29} with an emergent C- symmetry. We also analyze the symmetry breaking and the excitation spectrum in the SSS phase. Then as the boost increases further, there is a QPT from the SSS to the stripe solid with $z = 2$. The resulting stripe solid may have vacancies whose BEC leads to the SSS from the stripe solid side. We show that the driving a superfluid is a new and effective mechanism to generate a supersolid which is a long time elusive goal in low temperature physics and can be realized not only in $\text{He}4$, but also in various cold atom systems with long-range dipole-dipole interactions, spin-orbit couplings or dressed by Rydberg atoms.

2. Co-moving frame and the lab frame in a running SF

In the co-moving frame with the SF, the SF is static. In terms of the SF order parameter $\psi = \sqrt{\rho_0 + \delta\rho}e^{i\phi}$, one just takes the effective action inside the SF phase⁴⁹:

$$\mathcal{L}_{M:SF}[\delta\rho, \phi] = i\delta\rho\partial_\tau\phi + \rho_0[v_x^2(\partial_x\phi)^2 + v_y^2(\partial_y\phi)^2] + u(\delta\rho)^2 + w\rho_0(\partial_y\phi)^3 + \dots \quad (1)$$

where, in addition to phase-magnitude conjugation $i\delta\rho\partial_\tau\phi$, the last cubic derivative term also breaks the Charge conjugation (C-) symmetry $\phi \rightarrow -\phi, \delta\rho \rightarrow -\delta\rho$ in the $(\delta\rho, \phi)$ representation $[\delta\rho, \phi] = i\hbar$.

Now one gets to the lab frame just by performing a Galileo transformation (GT)^{9,29} (see also the appendix A for an independent microscopic calculation) $\partial_\tau \rightarrow \partial_\tau - ic\partial_y$ (we drop the '):

$$\mathcal{L}_{L:SF}[\delta\rho, \phi] = i\delta\rho\partial_\tau\phi + \rho_0[v_x^2(\partial_x\phi)^2 + v_y^2(\partial_y\phi)^2] + u(\delta\rho)^2 + w\rho_0(\partial_y\phi)^3 + c\delta\rho\partial_y\phi \quad (2)$$

where the boost velocity was pinned to be $\vec{c} = \vec{Q}/m$.

The order parameter in the lab frame becomes

$$\psi_{SF} = \sqrt{\rho_0 + \delta\rho}e^{i(\vec{Q}\cdot\vec{x} + \phi)} \quad (3)$$

which carries a SF flow in the lab frame.

In the following, we will study the possible instability when the flow is beyond a critical one from both phase representation and its dual magnitude representation in the lab frame. The C- symmetry case was addressed in⁹ in a completely different context: a quantum magnet with SOC in a longitudinal Zeeman filed. The C- symmetry only exists in a lattice system at integer fillings^{9,29,32}. However, there is no C- symmetry in all the continuous SF systems mentioned in the introduction. It is the absence of the C- symmetry which leads to the new QPTs in all the following sections³³.

3. The quantum Lifshitz transition from the SF to the BSF driven by the instability in the Goldstone mode

Taking $\vec{c} = \vec{Q}/m$ as an independent tuning parameter, we will study the putative SF to the BSF transition tuned

by this boost. see also the appendix A for an independent microscopic calculation.

After integrating out the magnitude fluctuations in Eq.2, the quantum phase fluctuations are described by:

$$\mathcal{L}_{L:SF}[\phi] = \frac{1}{2u}(\partial_\tau\phi - ic\partial_x\phi)^2 + \rho_0[v_x^2(\partial_x\phi)^2 + v_y^2(\partial_y\phi)^2] + w\rho_0(\partial_y\phi)^3 \quad (4)$$

which has the Translational symmetry $\vec{x} \rightarrow \vec{x} + \vec{a}$ and the $U(1)_c$ symmetry $\phi \rightarrow \phi + \phi_0$.

Now we study how the SF evolves as one increases \vec{Q} . The mean-field state can be written as $\phi = \phi_0 + k_0 y$. Substituting it to the effective action Eq.4 leads to:

$$\mathcal{S}_0 \propto (2u\rho_0 v_y^2 - c^2)k_0^2 + 2w u \rho_0 k_0^3 \quad (5)$$

At a low boost $c^2 < 2U\rho_0 v_y^2$, $k_0 = 0$ is in the SF phase which breaks the $U(1)_c$ symmetry, but still keeps the translational symmetry. Its spectrum is given by:

$$\omega = \sqrt{2u\rho_0(v_x^2 k_x^2 + v_y^2 k_y^2)} - ck_y \quad (6)$$

At the critical boost between the SF and the boosted SF

$$c^2 = 2U\rho_0 v_y^2 = v_{c,p}^2 \quad (7)$$

which gives the phase boundary in Fig.3a. The physical meaning is clear: when the moving velocity of the SF matches that of the SF Goldstone mode. there is an instability to a new phase called boosted SF phase in the following.

At a high boost $c^2 > 2U\rho_0 v_y^2$

$$k_0 = \frac{c^2 - 2U\rho_0 v_y^2}{3wU\rho_0} \quad (8)$$

where $w = c$, so its sign is completely determined by the driving. So the BSF phase has an additional modulation k_0 along the y -axis on top of Eq.3:

$$\psi_{BSF} = \sqrt{\rho_0 + \delta\rho} e^{i[(\vec{Q} + \vec{k}_0) \cdot \vec{x} + \phi]} \quad (9)$$

which still keeps the diagonal symmetry $\vec{x} \rightarrow \vec{x} + \vec{a}$, $\phi \rightarrow \phi - \vec{k}_0 \cdot \vec{a}$. So the symmetry breaking is

$$U(1)_T \times U(1)_c \rightarrow [U(1)_T \times U(1)_c]_D \quad (10)$$

which still leads to one Goldstone mode.

Inside the BSF phase, the quantum phase fluctuations can be written as $\phi \rightarrow \phi_0 + k_0 y + \phi$. Expanding the action upto the second order in the phase fluctuations leads to

$$\mathcal{L}_{BSF} = (\partial_\tau\phi - ic\partial_y\phi)^2 + 2U\rho_0 v_x^2(\partial_x\phi)^2 + (2c^2 - 2U\rho_0 v_y^2)(\partial_y\phi)^2 + 2wU\rho_0(\partial_y\phi)^3 + b(\partial_y\phi)^4 + \dots \quad (11)$$

which leads to the gapless Goldstone mode inside the BSF phase:

$$\omega_{\mathbf{k}} = \sqrt{2U\rho_0 v_x^2 k_x^2 + (2c^2 - 2U\rho_0 v_y^2)k_y^2} - ck_y \quad (12)$$

where one can see $2c^2 - 2U\rho_0 v_y^2 = c^2 + (c^2 - 2U\rho_0 v_y^2) > c^2$ when $c^2 > 2U\rho_0 v_y^2$, thus the $\omega_{\mathbf{k}}$ is stable in BSF phase.

It is instructive to expand the first kinetic term in Eq.4 as:

$$2U\mathcal{L} = Z(\partial_\tau\phi)^2 - 2ic\partial_\tau\phi\partial_y\phi + 2U\rho_0 v_x^2(\partial_x\phi)^2 + \gamma(\partial_y\phi)^2 + a(\partial_y^2\phi)^2 + 2wU\rho_0(\partial_y\phi)^3 + b(\partial_y\phi)^4 \quad (13)$$

where Z is introduced to keep track of the renormalization of $(\partial_\tau\phi)^2$, $\gamma = 2U\rho_0 v_y^2 - c^2 = v_{c,p}^2 - c^2$ is the tuning parameter. By using the universal relation for the 2d superfluid density $\Delta\rho_s/k_B T_c = 2/\pi$, one can deduce the finite temperature critical temperature³⁰:

$$\frac{T_c}{T_{c0}} = |1 - (\frac{c}{v_{c,p}})^2| < 1 \quad (14)$$

initial part of which at a small Q is shown in Fig.3.

The scaling $\omega \sim k_y^3, k_x \sim k_y^2$ leads to the exotic dynamic exponents ($z_x = 3/2, z_y = 3$). Then one can get the scaling dimension of $[\gamma] = 2$ which is relevant, as expected, to tune the transition, but $[Z] = [b] = -2 < 0$, so are two leading irrelevant operators which determine the finite T behaviours and corrections to the leading scalings. However $[w] = 0$ is marginal. The standard field theory one-loop RG finds:

$$\frac{dw}{dl} = \epsilon w - Aw^3 \quad (15)$$

where $\epsilon = 2 - d$ and $A = 1/v_x^2 a > 0$. Note that the sign of w changes under the C - transformation $\phi \rightarrow -\phi$. So Eq.15 reduces to

$$\frac{d|w|}{dl} = \epsilon|w| - A|w|^3 \quad (16)$$

So it is marginally irrelevant at $d = 2$, simply irrelevant at $d = 3$. Setting $Z = w = 0$ in Eq.13 leads to the Gaussian fixed point action at the QCP where $\gamma = 0$, subject to the Logarithmic correction due to the marginally irrelevant w term. Again it is the crossing metric $g_{\tau,y} = g_{y,\tau} = -ic$ in Eq.13 which dictates the quantum dynamic scaling near the QCP. It is a direct reflection of the new emergent space-time near the $z = (3/2, 3)$ QPT. Note that here the QPT is a quantum Lifshitz one tuned by $[\gamma] = 2$, so despite the cubic derivative term $[w] = 0$, it could still be a 2nd -order transition in Fig.3a, in contrast to the conventional QPT where a cubic term drives a first order one.

Now we evaluate the conserved currents in both SF and BSF phase. The former symmetry breaking pattern is just $U(1)_c \rightarrow 1$. The latter is $U(1)_T \times U(1)_c \rightarrow [U(1)_T \times U(1)_c]_D$. Due to the different symmetry breaking pattern, it is a QPT from the SF to the BSF. Now

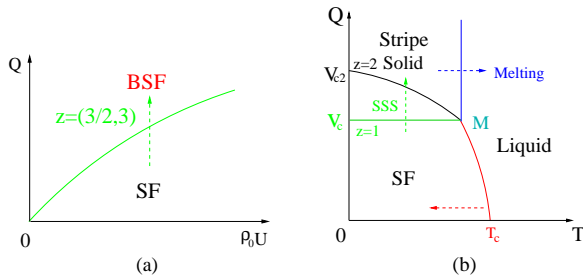


FIG. 3. The instabilities of driving a SF. (a) In the absence of a roton, the instability happens near the origin (the phonon mode), it leads to a BSF phase at $T = 0$. If there exists of a roton such as in He4, the instability at $k = 0$ will always be pre-empted by that near the roton at $k = k_0$. (b) The instability near the roton minimum leads to a stripe supersolid (SSS) phase at $T = 0$. $T_c \sim 2.13K$ at $Q = 0$ remains the same as in Fig.2a, but decreases as Eq.14 as Q increases. The critical velocity is estimated in Eq.30 as $v_c \sim 10m/s$. The QPT from the SF to the SSS is in the same universality class as that from the boosted Mott to the SF with $z = 1$ ^{9,29}. There is also a QPT from the SSS to the stripe solid with $z = 2$ at $v = v_{c2}$. The finite temperature melting transition from the stripe solid to the normal liquid at $T = T_M$ is also in the 3d XY universality class. The BEC of the vacancies in the stripe solid leads to the SSS intervening between the SF and the stripe solid. There is an emergent C- symmetry at $v = v_{c,d}$ dictating $z = 1$, but no C- symmetry away from the QCP. The order parameters in all the 4 phases are: Normal liquid $\langle \psi_0 \rangle = 0, \langle \psi_G \rangle = 0$, SF $\langle \psi_0 \rangle \neq 0, \langle \psi_G \rangle = 0$, Stripe solid $\langle \psi_0 \rangle = 0, \langle \psi_G \rangle \neq 0$, SSS $\langle \psi_0 \rangle \neq 0, \langle \psi_G \rangle \neq 0$.

we try to find an order parameter to distinguish the two phases. The $U(1)_c$ symmetry in the normal phase transpire as $\phi \rightarrow \phi + a$ for any shift a inside the $U(1)_c$ symmetry broken SF phase, so the Noether current can be derived from Eq.4 as:

$$\begin{aligned} J_\tau &= 2(\partial_\tau \phi - i c \partial_y \phi) \\ J_x &= 4u \rho_0 v_x^2 \partial_x \phi \\ \tilde{J}_y &= J_y - i c J_\tau = 2u \rho_0 [2v_y^2 (\partial_y \phi) + 3w (\partial_y \phi)^2] - i c J_\tau \end{aligned} \quad (17)$$

In the SF phase, $\phi = \phi_0$, then $(J_\tau, J_x, \tilde{J}_y) = (0, 0, 0)$ and $(J_\tau, J_x, J_y) = (0, 0, 0)$ also. In the BSF phase, $\phi = \phi_0 + k_0 y$ where k_0 is given by Eq.8, then $(J_\tau, J_x, \tilde{J}_y) = (-i 2c k_0, 0, 0)$, but $(J_\tau, J_x, J_y) = (-i 2c k_0, 0, 2c^2 k_0)$. So the conserved currents (J_τ, J_x, J_y) can still be used to distinguish the BSF from the SF phase.

However, if there exists roton shown in Fig.2c, then this SF to BSF transition will be preempted by the the SF to a solid transition triggered by the roton touchdown as shown in the following sections.

4. The SF to the SF density wave transition driven by the instability in the roton mode

In Helium 4, due to the long-range Wan der-Waals interaction, the density-density interaction $V_d(q)$ develops a roton minimum which drives the transition from the SF to a solid²⁰. Now the density-density interaction U

becomes long-ranged in Helium 4, so we adopt the notation in⁴⁹ as $U = V_d(k) = a - b k^2 + \alpha k^4$ which can be written as $V_d(k) = \Delta + \alpha(k^2 - k_0^2)^2$ near the roton minimum (Fig.2c). We also consider the isotropic case $v_x^2 = v_y^2$, then $\rho_s = \rho_0 v_x^2 = \rho_0 v_y^2$ is the superfluid density, $\kappa^{-1} = \lim_{k \rightarrow 0} V_d(k) = a$ is the compressibility and $v^2(k) = \rho_s V_d(k)$.

From Eq.3, one can see that the density stays the same in both the lab frame and the co-moving frame. The dynamic structure factor is:

$$S_n^>(\vec{k}, \omega) = S_n(\vec{k}) \delta(\omega - \epsilon_+(\vec{k})), \quad S_n(\vec{k}) = \frac{\pi \rho_s k}{2v(k)} \quad (18)$$

where $\epsilon_+(\vec{k}) = v(k)k + ck_x$ is the quasi-particle excitation energy.

It is easy to see that a generalized Feynmann relation still holds under the driving:

$$\epsilon_+(\vec{k}) = \frac{\int_0^\infty d\omega \omega S_n^>(\vec{k}, \omega)}{\int_0^\infty d\omega S_n^>(\vec{k}, \omega)} \quad (19)$$

A similar relation for the quasi-hole excitation energy $\epsilon_-(\vec{k}) = v(k)k - ck_x$ can be derived by replacing $S_n^>(\vec{k}, \omega)$ by $S_n^<(\vec{k}, \omega)$.

After integrating out the phase fluctuations in Eq.2, the quantum magnitude fluctuations can be used to describe such a transition under a driving:

$$\begin{aligned} \mathcal{L}[\delta\rho] &= \frac{1}{2} \delta\rho(-k, -\omega) \left[\frac{\omega^2 + i 2c \omega k_x}{\rho_s k^2} + (\Delta - \frac{c^2 k_x^2}{\rho_s k^2}) \right. \\ &\quad \left. + \alpha(k^2 - k_0^2)^2 \right] \delta\rho(k, \omega) - w(\delta\rho)^3 + u(\delta\rho)^4 + \dots \end{aligned} \quad (20)$$

where r is the roton gap near $k = k_0$. Again the cubic term in the density-density channel need to be included at the very beginning.

The U term nails down the momentum k to be in the roton ring $k = k_0$, the boost term pins it to be in the k_x axis $k_x = \pm k_0$. So the boost term just introduce an easy-axis to the isotropic roton mode. So the resulting solid has only two shortest reciprocal lattice vectors $\vec{G} = \pm k_0 \hat{x}$:

$$\begin{aligned} n &= n_0 + (\psi_G e^{ik_0 x} + \psi_G^* e^{-ik_0 x}) \\ &= n_0 + 2|\psi_G| \cos(k_0 x + \alpha) \end{aligned} \quad (21)$$

where ψ_G is the complex order parameter. Its phase α is the gapless phonon mode due to the translational symmetry breaking. It is the stripe solid phase. In fact, as shown in³⁶, even without such an easy axis term which explicitly breaks the rotational symmetry, a strip solid phase is most likely to be the ground state lattice structure due to the spontaneously lattice symmetry breaking. In the presence of such an easy axis term, the stripe solid is the ground state.

Then writing $k_x = \pm k_0 + q_x, k_y = q_y$ and expanding up to the quartic term, we obtain:

$$\mathcal{L}[\delta\rho] = \frac{1}{2}\delta\rho(-\vec{q}, -\omega)[\frac{\omega^2 + i2c\omega q_x}{\rho_s k_0^2} + 4\alpha k_0^2 q_x^2 + \frac{c^2}{\rho_s k_0^2} q_y^2 + \tilde{r}\delta\rho(\vec{q}, \omega) - w(\delta\rho)^3 + u(\delta\rho)^4 + \dots] \quad (22)$$

where $\tilde{r} = \Delta - c^2/\rho_s$ is the boosted roton gap and $k_x = \pm k_0 + q_x, k_y = q_y$ need to be summed around both regimes near $\pm k_0$. Using the decomposition Eq.21, one obtain the effective action describing the SF to the stripe solid transition³⁸:

$$\mathcal{L}[\psi_G] = \frac{1}{2}\psi_G^*(\vec{q}, \omega)[\frac{\omega^2 + i2c\omega q_x}{\rho_s k_0^2} + 4\alpha k_0^2 q_x^2 + \frac{c^2}{\rho_s k_0^2} q_y^2 + \tilde{r}\psi_G(\vec{q}, \omega) + u|\psi_G|^4 + \dots] \quad (23)$$

where due to the stripe structure, the cubic term plays no role. In fact as shown in³⁶, the cubic term play an important role only in a triangular lattice where the three shortest reciprocal lattice vectors form a closed triangle.

Substituting Eq.21 into the original boson Eq.3, we get the corresponding order parameter for the superfluid density wave (SDW):

$$\psi_{SDW} = \sqrt{\rho_0}e^{i(\vec{Q}\cdot\vec{x}+\phi)}[1 + |\psi_G| \cos(k_0x + \alpha)/\rho_0] \quad (24)$$

which establishes the relation between the original boson ψ_{SDW} and the order parameter ψ_G in the effective action Eq.23. The translational symmetry $x \rightarrow x + a$ in Eq.21 translates into the $U(1)_T$ symmetry of $\psi_G \rightarrow \psi_G e^{ik_0a}$ where its phase $\theta = k_0a$ is any continuous real number³⁷. The $U(1)_T$ symmetry breaking leads to the Goldstone mode which is the phonon mode α in Eq.21 due to the translational symmetry breaking to the SDW phase. It breaks the $U(1)_T \times U(1)_c \rightarrow 1$ symmetry leading to the two Goldstone modes ϕ, α which are the superfluid and lattice Goldstone mode respectively.

Eq.23 can be rewritten as:

$$\mathcal{L}[\psi_G] = \frac{1}{2}\psi_G^*(\vec{q}, \omega)[\frac{(\omega + icq_x)^2 + (c^2 + 4\alpha\rho_s k_0^4)q_x^2}{\rho_s k_0^2} + \frac{c^2}{\rho_s k_0^2} q_y^2 + \tilde{r}\psi_G(\vec{q}, \omega) + u|\psi_G|^4 + \dots] \quad (25)$$

where $c^2 < c^2 + 4\alpha\rho_s k_0^4$, so it is nothing but in the same universality class of QPT from the boosted Mott to SF along the Path-I in Fig.3a in²⁹. The boost c is exactly marginal, so it is a boosted 4D XY model with the dynamic exponent $z_x = z_y = 1$. Despite the original action Eq.2 has no C-symmetry, it has an emergent C-symmetry in the effective action Eq.23.

Setting $\tilde{r} = \Delta - c^2/\rho_s = 0$ leads to a new critical velocity:

$$c^2 = \rho_s \Delta = v_{c,d}^2 \quad (26)$$

which gives the SF to the SDW phase boundary in Fig.3b. When $\tilde{r} > 0, \langle\psi_G\rangle = 0$, it is in the SF phase. When

$\tilde{r} < 0, \langle\psi_G\rangle \neq 0$, it is in the Stripe SF density wave (SFDW) phase. It is new because it only depends on the roton gap Δ , independent of its minimum k_0 .

The main differences between the BSF in Eq.9 and the SDW in Eq.24 is that in the former, it is a phase fluctuation ϕ driven QPT, so there is only one wavevector component $\vec{Q} + \vec{k}_0$. The symmetry breaking pattern is $U(1)_T \times U(1)_c \rightarrow [U(1)_T \times U(1)_c]_D$ which leads to only one gapless Goldstone mode ϕ , while in the latter, it is a magnitude fluctuation $\delta\rho$ driven QPT, so there are three wavevector components \vec{Q} and $\vec{Q} \pm \vec{k}_0$ which leads to the magnitude modulation in Eq.24. The symmetry breaking pattern is $U(1)_T \times U(1)_c \rightarrow 1$ which leads to two gapless Goldstone modes ϕ and α .

5. Crossover from the SDW to the stripe supersolid (SSS) and SSS to the stripe solid transition

Eq.24 holds near the SF to the SDW transition. As one increases the boost further, the superfluid density ρ_s starts to decrease as the normal solid component $|\psi_G|$ develops in Eq.21. Then the density order Eq.21 emerges as an independent order parameter. The SDW crossovers to the stripe supersolid (SSS). One can write down a GL theory⁴⁹ in terms of the two independent order parameters ψ and δn and their mutual couplings. For example, the periodic potential $\delta n = 2|\psi_G| \cos(k_0x + \alpha)$ in Eq.21 acts as a periodic potential $\delta n|\psi(x)|^2$ on the superfluid component ψ , so one can write down the generic expression for ψ :

$$\psi_{SSS} = \psi_0 e^{i\vec{Q}\cdot\vec{x}}[1 + A|\psi_G| \cos(k_0x + \alpha)] \quad (27)$$

where $\psi_0 = \sqrt{a}e^{i\phi}$ and A is a numerical factor of the order 1. Well inside the stripe supersolid, the coupling between the two gapless modes ϕ and α leads to two branches of supersolidons²⁰.

As the boost increase further, the normal solid component $|\psi_G|$ increases, the superfluid component ψ_{SSS} decreases and eventually disappears. There is a QPT from the SSS where $\langle\psi_0\rangle \neq 0, \langle\psi_G\rangle \neq 0$ (or equivalently $\langle\psi_{SSS}\rangle \neq 0, \langle\delta n\rangle \neq 0$) to the stripe solid $\langle\psi_0\rangle = 0, \langle\psi_G\rangle \neq 0$ (or equivalently $\langle\psi_{SSS}\rangle = 0, \langle\delta n\rangle \neq 0$) in Fig.3b. Just in terms of symmetry breaking, there is really no difference between the SDW and the SSS, so Eq.24 where $a \sim \rho_0$ and Eq.27 $a \ll \rho_0$ have the same symmetry breaking structure. But the former works best near the SF to the SDW transition described by Eq.23 with $z = 1$ where the SF component is non-critical (so does ρ_s in Eq.23). While the latter works best near the SSS to the stripe solid transition where the SF component becomes critical which is described by the $z = 2$ effective action³¹:

$$\mathcal{L}[\psi_0] = \psi_0^*(\vec{q}, \omega)[iZ_1\omega + v_x^2 q_x^2 + v_y^2 q_y^2 - \tilde{\mu}]\psi_0(\vec{q}, \omega) + u|\psi_0|^4 + \dots \quad (28)$$

where $\tilde{\mu} = v_{c2} - v$. It breaks the C-symmetry explicitly. The phenomenological parameters Z_1, v_x^2, v_y^2 depend on Q and k_0 in Fig.3b. Unfortunately, one is not able to

determine the numerical value of such $v_{c2} > v_c$ from the present effective action approach. At any finite $T < T_c$ in Fig.2b, the transition from the SSS to the stripe solid becomes a classical 3d XY one driven by the SF Goldstone mode ϕ . As the temperature increase further to T_c , there is a second transition from the stripe solid to the normal liquid described by Eq.29. It is also a classical 3d XY one, but driven by the phonon mode α .

It is constructive to compare with the extended boson Hubbard model^{27,28} where a stripe supersolid was shown to always exist slightly away from 1/2 filling both by microscopic calculations²²⁻²⁶ and effective actions in the original basis²²⁻²⁵ and the dual vortex basis^{27,28}. Due to the lack of C- symmetry, the vacancies usually have lower energies than that of interstitials, the stripe solid always host some vacancies. If their excitation energies E_v are positive, so can only be thermally excited. But when they become negative, they may undergo BEC. So approaching from the stripe solid side, the ψ_{SSS} in Eq.27 can be interpreted as the BEC of vacancies in the spontaneously formed stripe solid in Eq.21. The vacancies behave similarly as the holes on the top of the CDW or Valence Bond (VB) state at 1/2 filling examined in^{27,28} described by the effective action Eq.28 with $z = 2$.

6. Normal Liquid to stripe solid transitions.

In fact, by only keeping the $\omega = 0$ component in Eq.23, it may also be used to describe the normal liquid to stripe solid transition at a finite T in Fig.3b.

$$\begin{aligned} \mathcal{L}[\psi_G] = & \frac{1}{2}\psi_G^*(\vec{q}, \omega)[u_x^2q_x^2 + u_y^2(q_y^2 + q_z^2) + \tilde{r}]\psi_G(\vec{q}, \omega) \\ & + u|\psi_G|^4 + \dots \end{aligned} \quad (29)$$

where we used the 3d-space explicitly³⁸. When $\tilde{r} = T - T_c > 0$, $\langle \psi_G \rangle = 0$, it is in the normal liquid phase. $\langle n \rangle = n_0$. $\tilde{r} < 0$, $\langle \psi_G \rangle \neq 0$, it is in the Stripe solid phase still described by Eq.21 $\langle n \rangle = n_0 + 2|\psi_G| \cos(k_0 x + \alpha)$. It is in the 3d XY universality class. From the low temperature stripe solid side, it may also be understood as a stripe lattice melting transition driven by the phonons α from the low temperature stripe solid side which also leads to Eq.29. While, as stressed below Eq.28, the finite $T < T_c$ transition resulting from Eq.28 is a 3d class driven by the SF Goldstone mode ϕ .

7. Experimental realizations.

We study two kinds of instabilities: the one induced by the SF Goldstone mode near $k = 0$ in the absence of rotons and the one induced by the roton mode near $k = k_0$. Here we discuss their experimental realizations respectively.

Eq.7 shows that when the moving velocity of the SF matches that of the SF Goldstone mode. there is an instability to the BSF. The sound velocity in He4 is about $v_{SF} \sim 238m/s$. In a conventional lab on the earth, taking a high way (magnetic levitated) train moving with a velocity $300km/h \sim 83m/s$ is still below this characteristic velocity. A civil air-craft flight can reach even higher $800km/h \sim 240m/s$ which just reaches the sound

velocity in the Helium4. So the chance to see the instability near $k = 0$ is unlikely on the earth. As mentioned in the introduction, in addition to the well known SF in the He4, there are also excitonic SF in the electronic systems in semi-conductors. The Bilayer Quantum Hall systems (BLQH)⁴ hosts the exciton SF in the charge neutral sector with the Goldstone mode velocity $v_{BL} \sim 1.4 \times 10^4m/s$, The electron-hole bilayer system (EHBL)⁵ holds the exciton SF with $v_{EH} \sim 5 \times 10^3m/s$. It is essentially impossible except going to a satellite orbiting around the earth. The escape velocity of a satellite orbiting around the earth is $v_{esc} = 11.2km/s$. In this regard, the weakly interacting cold atom BEC systems^{2,3} become better candidates with the SF Goldstone mode velocity $v_{SF} \sim 1cm/s$.

Eq.26 shows that when the moving velocity of the SF is beyond a critical velocity determined by the roton gap, there is an instability to the stripe SS. Its value can be estimated as:

$$v_{c,d} = \sqrt{\frac{\Delta}{2m}} \sim 10m/s \quad (30)$$

where m is the He4 atom mass and $\Delta/k_B \sim 10K$ is the roton gap.

As mentioned in the introduction Fig.1a and reviewed in the appendix B-1, there is another critical velocity for an impurity moving in a superfluid. Its value due to the rotons in the He4 can be estimated by a simple Landau argument to be $v_{imp} \sim \frac{\Delta}{\hbar k_0} \sim 60m/s$ where $k_0 \sim 2\text{\AA}^{-1}$ is the momentum of the roton minimum. Our new critical velocity Eq.30 holds for a uniformly moving SF which is equivalent to a uniforming moving channel. Obviously a moving local heavy impurity is different from a moving channel holding the SF. Just from the general principle, we expect the critical velocity of the cases are different, but comparable $v_{imp} \sim v_{c,d}$. Our concrete calculations show that this is indeed the case due to $\Delta \sim \frac{\hbar^2 k_0^2}{2m} \sim 20K$.

It was also known that the critical velocity for the SF moving in a narrow channel with the width d can be empirically fitted to be $v_{ch} \sim \frac{\hbar}{md}$. We expect this form breaks down in an extremely narrow channel $d \rightarrow 0$ and also an extremely wide channel $d \rightarrow \infty$. Our new critical velocity Eq.30 holds for extremely wide channel $d \rightarrow \infty$

The SSS can be detected by the same NCRI experiments^{18,21}. The NCRI is proportional to the superfluid density which is, of course, anisotropic $\sim a^2 v_x^2$ if the rotational axis is along the boost direction \hat{x} , $\sim a^2 v_y^2$ if the rotational axis is normal to the boost direction \hat{x} . It will monotonically increases when moving from the SSS side near the $z = 2$ line to the SDW side with $z = 1$.

Therefore Fig.3 can be mapped out^{18,39} by driving the SF beyond the critical velocity in Eq.30. Cold atom BEC systems with a long-range interaction such as a dipole-dipole interaction⁴⁰⁻⁴³ or with spin-orbital couplings^{46,47} or dressed by Rydberg atoms^{44,45} may support rotons with much smaller critical velocities. So Fig.3 may find wide applications in these cold atom systems with tunable roton gaps.

8. Conclusions.

Obviously, the SF and the stripe solid phase break two completely different symmetries: In the former, it is the internal $U(1)_c$ symmetry whose breaking leads to the gapless Goldstone mode, in the latter, it is the translational symmetry whose breaking leads to the gapless lattice phonon modes. Just from general symmetry principle, there are two possibilities on the QPT from the SF to the solid: (1) a direct 1st order transition. This is the case driven by the pressure P in He4 in Fig.2a. The roton minima is rotationally symmetric. The QPT near $k = k_0$ is first order one driven by the pressure resulting a hcp solid structure, then the SF just disappears suddenly across the QPT. Of course, the first order transition indicates that there could also be a coexistence of SF and solid near the SF-Solid phase boundary resulting a phase separation. This is indeed the case confirmed by the refined PSU experiment²¹. In fact, as a retrospect, the SS phase, despite its tantalizing properties, should not be expected in such an environment in the very first place. (2) It splits into two second order ones with an intervening SS phase. As demonstrated in this manuscript, this is the case in the 3d He4 or cold atom BEC with tunable rotons driven by the boost in Fig.3b. The QPT near $k = k_0$ is second order one with $z = 1$ driven by the boost Q resulting a stripe solid component, then the SF undergoes an accompanying second order QPT to a superfluid density wave (SDW). The boost transfers the rotationally symmetric roton minima to just two opposite degenerate minima along the boost direction. The QPT is in the same universality class as the $z = 1$ boosted Mott-SF transition studied previously in a different context²⁹. Then the Stripe SDW evolves into the stripe supersolid phase where the solid component is given by $\delta\rho$, the superfluid density wave component is given by ψ_{SDW} . Finally the SSS phase gets into a stripe solid phase through the $z = 2$ QPT by kicking out of its SDW component ψ_{SDW} which stands for vacancies near the QPT from the stripe solid side. A microscopic calculation such as a QMC simulation is needed to confirm the existence of these vacancies and their stabilities against the phase separations. We expect that phase separations are usually associated with the first order transition such as in Fig.1a in the case (1), but not the second order one such as in Fig.2b in the case (2). If so, we may have discovered a new mechanism to realize a stable supersolid phase. Then the boost becomes an effective way to generate a supersolid which does not happen when increasing the pressure

This work was originally initiated by the author's earlier works^{20,49} on putative SS in He4. I thank Moses Chan for helpful discussions during the very early stage of this work. I also thank Fadi Sun for the collaborations on the two related works^{9,29} which inspired the author to get back to finish this early work.

Appendix A: A moving superfluid, Doppler shifts and Galileo transformation

In this appendix, we review the topic (2) mentioned in the introduction. we perform some microscopic Bogoliubov calculations to quadratic order on a moving superfluid to demonstrate the known phenomena of Doppler shifts due to the Galileo transformation. They are consistent with the mean field + Gaussian fluctuation analysis on the effective action approach used in the main text. However, the main limitation of the microscopic calculations used in this appendix is that it is not able to determine what is the quantum phase beyond the critical velocity, let alone the universality class of the quantum phase transitions driven by the boost. One must push this Bogoliubov calculations to infinite order to address this questions. This can only be achieved by the effective action and RG approach used in the main text.

1. Doppler shift in a moving SF at weak coupling:

The Hamiltonian for weakly interacting bosons in a continuum system such as the ESF in the EHBL^{5-7,54} is

$$H_B = \sum_{\vec{k}} (\epsilon_{\vec{k}} - \mu) b_{\vec{k}}^\dagger b_{\vec{k}} + \frac{1}{2A} \sum_{\vec{k}, \vec{p}, \vec{q}} V(\vec{q}) b_{\vec{k}-\vec{q}}^\dagger b_{\vec{p}+\vec{q}}^\dagger b_{\vec{p}} b_{\vec{k}} \quad (A1)$$

where $\epsilon_{\vec{k}} = \hbar^2 k^2 / 2m$ is the free boson dispersion, μ is the chemical potential, A is the 2d area, $V_d(\vec{q})$ is the boson-boson interaction. We assume it is weak, so the following Bogoliubov method applies.

Setting the SF moving with a momentum \vec{Q} :

$$\psi_0 = \sqrt{N_0} e^{i\vec{Q} \cdot \vec{x}} \quad (A2)$$

which means a finite superflow $\vec{v} = \vec{Q}/m$ where m is the mass of an atom. Now one can write the boson operator as:

$$\psi_{\vec{Q}+\vec{k}} = \sqrt{N_0} \delta_{\vec{k},0} + b_{\vec{Q}+\vec{k}} \quad (A3)$$

where $b_{\vec{Q}+\vec{k}}$ stands for the quantum fluctuations with the momentum \vec{k} measured relative to the BEC momentum \vec{Q} .

Substituting Eq.A3 into Eq.A1 and expanding it to the quadratic order, one can determine the chemical potential μ by eliminating the linear term of $b_{\vec{Q}}$ in the Hamiltonian H_{SF} as

$$\mu = n_0 V_d(0) + \frac{1}{2} m v^2 \quad (A4)$$

where $n_0 = N_0/A$ is the condensate density. Then one obtain the mean field Hamiltonian H_{SF} to the quadratic order:

$$H_{SF} = \sum_{\vec{k}} [\epsilon_{\vec{k}} + n_0 V_d(\vec{Q} - \vec{k}) - \epsilon_{\vec{Q}}] b_{\vec{k}}^\dagger b_{\vec{k}} + \frac{n_0}{2} \sum_{\vec{k}} [V_d(\vec{k}) b_{\vec{Q}+\vec{k}}^\dagger b_{\vec{Q}-\vec{k}}^\dagger + h.c.] \quad (A5)$$

which can be diagonalized by the Bogoliubov transformation

$$\beta_{\vec{k}} = u_{\vec{k}} b_{\vec{Q}+\vec{k}} + v_{\vec{k}} b_{\vec{Q}-\vec{k}}^\dagger \quad (\text{A6})$$

We obtain H_{SF} in terms of the quasi-particle creation and annihilation operators $\beta_{\vec{k}}$ and $\beta_{\vec{k}}^\dagger$:

$$H_{SF} = E(0) + \sum_{\vec{k}} E_v(\vec{k}) \beta_{\vec{k}}^\dagger \beta_{\vec{k}} \quad (\text{A7})$$

where $E(0)$ is the ground state energy and

$$\begin{aligned} u_{\vec{k}}^2 &= \frac{\epsilon_{\vec{k}} + n_0 V_d(\vec{k})}{2E(\vec{k})} + \frac{1}{2} \\ v_{\vec{k}}^2 &= \frac{\epsilon_{\vec{k}} + n_0 V_d(\vec{k})}{2E(\vec{k})} - \frac{1}{2} \\ E_v(\vec{k}) &= E(\vec{k}) + \vec{k} \cdot \vec{v} \end{aligned} \quad (\text{A8})$$

$$\text{where } E(\vec{k}) = \sqrt{\epsilon_{\vec{k}}^2 + 2n_0 V_d(\vec{k}) \epsilon_{\vec{k}}}.$$

One can see that in the moving SF, $u_{\vec{k}}$ and $v_{\vec{k}}$ are the same as in the lab frame. However, the energy spectrum $E_v(\vec{k})$ contains a Doppler shift term $\vec{k} \cdot \vec{v}$ ^{50,51}. In the low energy limit $\vec{k} \rightarrow 0$ limit, $E_v(\vec{k}) \rightarrow u|\vec{k}| + \vec{k} \cdot \vec{v}$ where $u = \hbar \sqrt{\frac{n_0 V_d(0)}{m}}$ which is identical to Eq.7. If one picks up $\vec{k}|| - \vec{v}$, one can identify the critical velocity $v_c = u$. Unfortunately, as stressed in the first paragraph, one is not able to tell what will happen beyond the critical velocity from this Bogliubov approach. This outstanding problem can only be addressed by the effective action and RG approach demonstrated in the main text.

One can also obtain normal and anomalous Green function:

$$\begin{aligned} G_n(\vec{Q}; \vec{k}, \omega) &= i \frac{\omega - \vec{k} \cdot \vec{v} + \epsilon_{\vec{k}} + n_0 V_d(\vec{k})}{(\omega - \vec{k} \cdot \vec{v})^2 - E^2(\vec{k})} \\ G_a(\vec{Q}; \vec{k}, \omega) &= i \frac{n_0 V_d(\vec{k})}{(\omega - \vec{k} \cdot \vec{v})^2 - E^2(\vec{k})} \end{aligned} \quad (\text{A9})$$

where one can identify the excitation spectrum $\omega = \pm E(\vec{k}) + \vec{k} \cdot \vec{v}$ which is nothing but the last equation in Eq.A8.

2. Galileo transformation on the SF

The Galileo transformation is:

$$\begin{aligned} \vec{k}' &= \vec{k} \\ E' &= E - \vec{k} \cdot \vec{v} + \frac{1}{2} m v^2 \\ \mu' &= \mu + \frac{1}{2} m v^2 \end{aligned} \quad (\text{A10})$$

where \vec{k}', E', μ' are the momentum, energy and chemical potential in the moving frame, where \vec{k}, E, μ are those in the lab frame. Note that the momentum does not change, because as listed in Eq.A3, it was measured from the BEC momentum $\vec{Q} = m\vec{v}$ from very beginning.

In the moving frame, the Green functions take the same form as those in the lab frame:

$$\begin{aligned} G_n(\vec{k}', \omega') &= i \frac{\omega' + \epsilon_{\vec{k}'} + n_0 V_d(\vec{k}')}{\omega'^2 - E^2(\vec{k}')} \\ G_a(\vec{k}', \omega') &= i \frac{n_0 V_d(\vec{k}')}{\omega'^2 - E^2(\vec{k}')} \end{aligned} \quad (\text{A11})$$

By substituting

$$\omega' = E' - \mu' = E - \mu - \vec{k} \cdot \vec{v} = \omega - \vec{k} \cdot \vec{v} \quad (\text{A12})$$

which is just the non-relativistic $c_l \rightarrow \infty$ limit of a relativistic Doppler shift, one can see Eq.A11 recovers Eq.A9.

It would be interesting to look at how the photons are emitted from the moving ESF in the EHBL systems^{5-7,54}, especially across the QPT from the SF to the BSF in Fig.3a at both $T = 0$ and a finite T . As warned above, the Bogliubov method here may not be applied near any QPTs. One may extend the effective action developed in Sec.2 in the main text to couple to a photon bath to achieve this goal. This approach can also be applied to study the chiral edge state of a FQH phase⁵⁶.

Appendix B: Driving a classical object through a superfluid

In the last two subsections, we drive the quantum fluids, no classical objects embedded inside it. In this section, we study the case of driving a classical object through a continuous fluid sketched in Fig.1a. It is a different class than that discussed in the main text, because here has both a classical object such as an impurity and the quantum fluid, while there is only quantum fluid in the latter. By analyzing how the GT act differently in the two cases, we also stress the crucial differences than the problems addressed in the main text. When above a critical velocity, these classical objects will all cause viscosities and dissipations. The three kinds of classical objects: a point impurity, an underlying optical lattice or a straight wall correspond to different space symmetry: a spherical, translation by a lattice constant or translational symmetry along the wall, so should lead to different critical velocities. Unfortunately, we are not able to provide any concrete solutions to such a different class of problems but we outline possible approach to solve such a different class of problems. As long as there are relative motions between the quantum fluids and the classical objects, it does not matter if it is the classical object moving or the quantum fluid moving, both need to the same physics. So in the following, we assume it is the classical object which is moving.

We start from a general Hamiltonian

$$\begin{aligned} \mathcal{H} &= \int d^2 x \psi^\dagger(\vec{x}) \left[-\frac{\hbar^2}{2m} \nabla^2 + V_1(\vec{x}) - \mu \right] \psi(\vec{x}) \\ &+ \int d^2 x_1 d^2 x_2 \psi^\dagger(\vec{x}_1) \psi(\vec{x}_1) V_2(x_1 - x_2) \psi^\dagger(\vec{x}_2) \psi(\vec{x}_2) \end{aligned} \quad (\text{B1})$$

where the single-body lattice potential $V_1(\vec{x})$ and the two-body interaction $V_2(x_1 - x_2)$ are automatically incorporated into the kinetic term and the interaction term respectively. By adding the chemical potential μ , we also change the canonical ensemble with a fixed number of particles N in the first quantization to the grand canonical ensemble in the second quantization. In the following, to simplify the notation, we use $V_{int} = \int d^2x_1 d^2x_2 \psi^\dagger(\vec{x}_1) \psi(\vec{x}_1) V_2(x_1 - x_2) \psi^\dagger(\vec{x}_2) \psi(\vec{x}_2)$.

1. A moving impurity

In a continuous system with a translational invariance, $V_1(x) = 0$ in Eq.B1. We look at the case of driving the impurity with a given velocity v in the Hamiltonian Eq.B1:

$$\mathcal{H}_L^i = \int d^2x \psi^\dagger(\vec{x}) \left[-\frac{\hbar^2}{2m} \nabla^2 - \mu - g_i \delta(\vec{x} - \vec{R} + \vec{v}t) \right] \psi(\vec{x}) + V_{int} \quad (B2)$$

where \vec{R} is the initial position, \vec{v} is the velocity of the impurity, g_i is the scattering potential strength. As expected, it is a time-dependent driving system in the lab frame.

In the frame moving together with the impurity⁵³, one can setting $\vec{x}' = \vec{x} + \vec{v}t$. Then one obtain the Hamiltonian in this co-moving frame (still drop the ' for the notational simplicity):

$$\mathcal{H}_M^i = \int d^2x \psi^\dagger(\vec{x}) \left[-\frac{\hbar^2}{2m} \nabla^2 - \mu - g_i \delta(\vec{x} - \vec{R}) - iv \partial_x \right] \psi(\vec{x}) + V_{int} \quad (B3)$$

which, as expected, becomes time-independent in the moving frame. Unfortunately, even so, it becomes very difficult to solve Eq.B3 even in such a static frame. It belongs to a quantum impurity problem⁵² where one need to deal with an impurity scattering on a moving fluid. If setting $g_i = 0$, the system is a gapless system describing by a CFT, then $g_i \neq 0$ may act as a Boundary condition changing operator in such a boundary CFT. The $g_i \rightarrow \infty$ limit may just directly set the Dirichlet boundary condition $\psi(\vec{x} = \vec{R}) = 0$. After solving such a quantum impurity problem in the static frame, one need to transfer the solution back to the lab frame where it becomes a time-dependent again. The earliest theoretical treatment is Landau's original argument by treating the impurity as a heavy classical particle and the quantum fluids as classical also which leads to $v_{im} \sim \Delta/k_0$. But such a classical treatment may not be precise to describe such a quantum impurity problem (for a more recent study, see¹⁶). It may break down in the presence of lattice anyway.

2. A moving optical lattice

Driving the underlying ionic lattice in a solid is hard to achieve in materials, but may be implemented in cold atom systems. It is easy to extend a single impurity located at position \vec{R} to a macroscopic lattice located at the ordered array of \vec{R}_i , so $V_1(\vec{x}) = \sum_{\vec{R}} v(\vec{x} - \vec{R})$ is a single-body attractive trapping potential. We look at

the case of driving the lattice at a given velocity v in the Hamiltonian Eq.B1:

$$\mathcal{H}_L^{OL} = \int d^2x \psi^\dagger(\vec{x}) \left[-\frac{\hbar^2}{2m} \nabla^2 - \mu - \sum_{\vec{R}} v(\vec{x} - \vec{R} + \vec{v}t) \right] \psi(\vec{x}) + V_{int} \quad (B4)$$

where \vec{R}_i are the initial positions of the ions, \vec{v} is the driving velocity of the lattice. As expected, it is a time-dependent driving lattice system in the lab frame.

In the frame moving together with the optical lattice, one can set $\vec{x}' = \vec{x} + \vec{v}t$. Then one obtain the Hamiltonian in this co-moving frame (still drop the ' for the notational simplicity):

$$\mathcal{H}_M^{OL} = \int d^2x \psi^\dagger(\vec{x}) \left[-\frac{\hbar^2}{2m} \nabla^2 - \mu - \sum_{\vec{R}} v(\vec{x} - \vec{R}) - iv \partial_x \right] \psi(\vec{x}) + V_{int} \quad (B5)$$

which, as expected, becomes time-independent in the moving frame.

The most dramatic differences between Eq.B1 with $V_1(x) = \sum_{\vec{R}} v(\vec{x} - \vec{R})$ and the current driving lattice case is that in the former one boost both the quantum and classical degree of freedoms at the same speed, so the relative distance between the boson and any lattice site $\vec{x}' - \vec{R}' = \vec{x} - \vec{R}$ is invariant under the GT, so it is a time-independent problem in any inertial frame. so it can be set to be zero in the tight-binding limit $\vec{x}' - \vec{R}' = \vec{x} - \vec{R} \rightarrow 0$ in any inertial frame. but here \vec{R}_i are just a array of constants, so invariant under the GT, but the relative distance between the boson and the lattice site $\vec{x} - \vec{R} + \vec{v}t$ is not invariant under the GT. It is time-independent in the co-moving frame, but becomes time-dependent in the lab frame. So even one may be able to take the time-binding limit in the former, it breaks down in the latter. Due to this fact, it becomes very difficult to solve Eq.B3 even in such a static frame. Then one need to transfer back the solution to the lab frame where it becomes a time-dependent problem again. So far, there is not any controlled theoretical treatment on such class of problems.

3. A moving straight hard wall along the x-axis

It is easy to extend the macroscopic lattice located at \vec{R}_i to a continuous wall, so $V_1(\vec{x}) = \int d\vec{R} v(\vec{x} - \vec{R})$ with the repulsive interaction $v(\vec{x} - \vec{R})$.

$$\mathcal{H}_L^W = \int d^2x \psi^\dagger(\vec{x}) \left[-\frac{\hbar^2}{2m} \nabla^2 - \mu - \int d\vec{R} v(\vec{x} - \vec{R} + \vec{v}t) \right] \psi(\vec{x}) + V_{int} \quad (B6)$$

where the continuous \vec{R} are the initial positions of the wall, \vec{v} is the velocity of the wall. As first glance, it seems a time-dependent driving system in the lab frame. A second look finds that by changing the variable $\vec{R}' = \vec{R} - \vec{v}t$, it becomes $\int d\vec{R} v(\vec{x} - \vec{R} + \vec{v}t) = \int d\vec{R}' v(\vec{x} - \vec{R}') = V_1(\vec{x})$ which is actually time-independent.

In the frame moving together with the wall, one can set $\vec{x}' = \vec{x} + \vec{v}t$. Then one obtain the Hamiltonian in this co-moving frame (still drop the $'$ for the notational simplicity):

$$\mathcal{H}_M^W = \int d^2x \psi^\dagger(\vec{x}) \left[-\frac{\hbar^2}{2m} \nabla^2 - \mu - \int d\vec{R} v(\vec{x} - \vec{R}) - iv\partial_x \right] \psi(\vec{x}) + V_{int}$$

which, as expected, becomes time-independent in the co-moving frame. Now if one takes the hard wall limit $v(\vec{x} - \vec{R}) \rightarrow \infty$ in the co-moving frame, then it just sets the boundary condition at the wall $\psi(\vec{x} = W) = 0$. One need to solve Eq.B7 with such a Dirichlet boundary con-

dition in such a static frame. Then one need to transfer back the solution to the lab frame which, as explained above, is still a time-independent problem⁵⁵. When the wall is very wide, it is equivalent to the moving SF case discussed in the main text. Eq.B6 and Eq.B7 formally looks the same, however, the SF phase is a $U(1)$ symmetry breaking phase where even the number of particles is (B7) not conserved. Then it gets back to the effective action treatments developed in the main text. This is another example of “ More is different ” enriched in²⁹. Our new critical velocity Eq.30 presented in the main text holds for a extremely wide channel $d \rightarrow \infty$ where the Dirichlet boundary condition does not affect the bulk.

¹ Anderson, Philip W. (1997) [1984]. Basic notions of condensed matter physics. Reading, Massachusetts: Addison-Wesley. ISBN 9780201328301.

² K. B. Davis, M. -O. Mewes, M. R. Andrews, N. J. van Druten, D. S. Durfee, D. M. Kurn, and W. Ketterle, Bose-Einstein Condensation in a Gas of Sodium Atoms, *Phys. Rev. Lett.* **75**, 3969 (1995) - Published 27 November 1995

³ M. W. Zwierlein, C. A. Stan, C. H. Schunck, S. M. F. Raupach, A. J. Kerman, and W. Ketterle, Condensation of Pairs of Fermionic Atoms near a Feshbach Resonance, *Phys. Rev. Lett.* **92**, 120403 (2004) - Published 25 March 2004

⁴ Longhua Jiang and Jinwu Ye, Ground state, quasi-hole and a pair of quasi-hole wavefunctions in Bi-layer Quantum Hall systems, *Phys. Rev. B* **74**, 245311 (2006).

⁵ Jinwu Ye, T. Shi and Longhua Jiang, Angle resolved Photoluminescence spectrum from exciton condensate in electron-hole semiconductor bilayers, *Phys. Rev. Lett.* **103**, 177401 (2009).

⁶ T. Shi, Longhua Jiang and Jinwu Ye, Two mode squeezing and photon statistics from exciton condensate, *Phys. Rev. B* **81**, 235402 (2010).

⁷ Jinwu Ye, Fadi Sun, Yi-Xiang Yu and Wuming Liu, Exciton correlations and input-out relations in non-equilibrium exciton superfluids, *Ann. Phys.* **329** (2013), 5172

⁸ Subir Sachdev, T. Senthil, and R. Shankar, Finite-temperature properties of quantum antiferromagnets in a uniform magnetic field in one and two dimensions, *Phys. Rev. B* **50**, 258 (1994).

⁹ Fadi Sun and Jinwu Ye, Response of a strongly interacting spin-orbit coupling system to a Zeeman field long version arXiv:2011.11287, version 2.

¹⁰ Jongchul Mun, Patrick Medley, Gretchen K. Campbell, Luis G. Marcassa, David E. Pritchard, and Wolfgang Ketterle, Phase Diagram for a Bose-Einstein Condensate Moving in an Optical Lattice, *Phys. Rev. Lett.* **99**, 150604 (2007) - Published 12 October 2007

¹¹ L. D. Landau, *J. Phys. USSR* **5**, 71 (1941)

¹² R. P. Feynman, "Progress in Low- Temperature Physics ", *loc. cit*

¹³ J. S. Langer and Michael E. Fisher, Intrinsic Critical Velocity of a Superfluid, *Phys. Rev. Lett.* **19**, 560 Published 4 September 1967

¹⁴ For a review, see A.L. Fetter and J. D. Walecka, *Quantum Theory of many-particle Systems*, Dover Publications, Inc. Mineola, New York, 2002.

¹⁵ G. E. Astrakharchik and L. P. Pitaevskii, Motion of a heavy impurity through a Bose-Einstein condensate, *Phys. Rev. A* **70**, 013608 (2004) - Published 20 July 2004

¹⁶ Gordon Baym and C. J. Pethick, Landau critical velocity in weakly interacting Bose gases, *Phys. Rev. A* **86**, 023602 Published 2 August 2012

¹⁷ A. Andreev and I. Lifshitz, *Sov. Phys. JETP* **29**, 1107 (1969); G. V. Chester, *Phys. Rev. A* **2**, 256 (1970); A. J. Leggett, *Phys. Rev. Lett.* **25**, 1543 (1970); W. M. Saslow , *Phys. Rev. Lett.* **36**, 1151?1154 (1976).

¹⁸ E. Kim and M. H. W. Chan, *Nature* **427**, 225 - 227 (15 Jan 2004), E. Kim and M. H. W. Chan, *Science* **24** September 2004; 305: 1941-1944,

¹⁹ For a collection of theoretical and experimental works inspired by Chan's experimental results, see a sepcial issue in *Journal of Low Temperature Physics*, 2012, edited by..... It also includes the author's²⁰.

²⁰ Yu Chen, Jinwu Ye and Quang Shan Tian, Classification of a supersolid: Symmetry breaking and Excitation spectra, *Journal of Low Temperature Physics*: **169** (2012), 149-168.

²¹ Duk Y. Kim and Moses H. W. Chan, Absence of Supersolidity in Solid Helium in Porous Vycor Glass, *Phys. Rev. Lett.* **109**, 155301 Published 8 October 2012.

²² G. Murthy, D. Arovas, and A. Auerbach, *Phys. Rev. B* **55**, 3104 (1997).

²³ R. G. Melko, *et al*, *Phys. Rev. Lett.* **95**, 127207 (2005).

²⁴ D. Heidarian and K. Damle, *Phys. Rev. Lett.* **95**, 127206 (2005);

²⁵ S. Wessel and M. Troyer, *Phys. Rev. Lett.* **95**, 127205 (2005).

²⁶ Jing Yu Gan, Yu Chuan Wen, Jinwu Ye, Tao Li, Shi-Jie Yang, Yue Yu, *Phys. Rev. B* **75**, 214509 (2007).

²⁷ Jinwu Ye, Duality, magnetic space group and their applications to quantum phases and phase transitions on bipartite lattices in several experimental systems. *Nucl. Phys. B* **805**, 418 (2008). here, we also find a new kind of supersolid called valenced bond supersolid (VB-SS). It only exists in a lattice system, not in any continuous system.

²⁸ Jinwu Ye and Chen Yan, Quantum phases, Supersolids and quantum phase transitions of interacting bosons in frustrated lattices, *Nucl. Phys. B* **869** (2013), 242-281

²⁹ Fadi Sun and Jinwu Ye, Emergent space-time near Quan-

tum Phase transitions, arXiv:2207.10475. V3.

³⁰ It is interesting to compare this relation with that of the finite temperature phase transition in the SF side of the SF-Mott quantum phase transition in a lattice observed in a moving frame with the velocity v studied in²⁹: $\frac{T_c}{T_{c0}} = \sqrt{1 + (\frac{v}{v_c})^2} > 1$. It is the lattice which makes the dramatic difference between the two formulas.

³¹ This $z = 2$ vacancy induced transition can be compared to the appearance of the $z = 2$ transition line in the boosted $z = 1$ SF-Mott transition presented in²⁹. After extracting out the modulation factor, then the $z = 1$ line transfers to the $z = 2$ line.

³² Fisher M. P. A., Weichman P. B., Grinstein G. and Fisher D. S., Phys. Rev. B 40, 546 (1989).

³³ For example, in the C-symmetry case, the phase and magnitude in Eq.1 are not conjugate variables anymore. In fact, they become independent, the magnitude mode becomes an independent Higgs mode. See^{9,29} for details.

³⁴ Fadi Sun, Jinwu Ye, Wu-Ming Liu, Fermionic Hubbard model with Rashba or Dresselhaus spinorbit coupling, New J. Phys. 19, 063025 (2017).

³⁵ Here, we only use the mean field ground state for the SF or BSF. In fact, as shown in⁴ in the context of exciton SF in BLQH and³⁴ in the context of a Y-y magnetic state in an fermionic SOC system, the mean field ground state will be modified by the quantum fluctuations in the ground state which is determined by the excitation spectrum even at $T = 0$.

³⁶ Longhua Jiang and Jinwu Ye, Lattice structures of Larkin-Ovchinnikov-Fulde - Ferrell (LOFF) state, Phys. Rev. B 76, 184104 (2007).

³⁷ It maybe constructive to compare the lattice phonon mode here with that in a lattice mode represented in⁹, here a in $x \rightarrow x + a$ is any real number, the k_0 is also any real number, then $\theta = k_0 a$ is a continuous number, it comes from a continuous translation symmetry breaking to a lattice translation normal to the stripe resulting the lattice phonon mode. While in the lattice $x \rightarrow x + a$ where a must be a lattice constant, $k_0 a$ is a continuous number only when k_0 is an In-commensurate number. it comes from the discrete lattice translation symmetry $x \rightarrow x + a$ breaking to none resulting the gapless phason mode.

³⁸ Here, we use the $2 + 1$ d notation. Due to the rotation symmetry around the boost x-axis (in the YZ plane), one may just set $q_y^2 \rightarrow q_y^2 + q_z^2$ in the 3d He4 case.

³⁹ Jacques Bossy, Jonathan V. Pearce, Helmut Schober, and Henry R. Glyde, Phonon-Roton Modes and Localized Bose-Einstein Condensation in Liquid Helium under Pressure in Nanoporous Media, Phys. Rev. Lett. 101, 025301 (2008) - Published 11 July 2008

⁴⁰ P. B. Blakie, D. Baillie, and R. N. Bisset, Roton spectroscopy in a harmonically trapped dipolar Bose-Einstein condensate, Phys. Rev. A 86, 021604(R) (2012) - Published 15 August 2012

⁴¹ D. Petter, G. Natale, R.M.W. van Bijnen, A. Patscheider, M.J. Mark, L. Chomaz, and F. Ferlaino, Probing the Roton Excitation Spectrum of a Stable Dipolar Bose Gas, Phys. Rev. Lett. 122, 183401 (2019) - Published 8 May 2019

⁴² John P. Corson, Ryan M. Wilson, and John L. Bohn, Stabilty spectroscopy of rotons in a dipolar Bose gas, Phys. Rev. A 87, 051605(R) (2013) - Published 21 May 2013

⁴³ R. N. Bisset, D. Baillie, and P. B. Blakie, Roton excitations in a trapped dipolar Bose-Einstein condensate, Phys. Rev. A 88, 043606 (2013) - Published 7 October 2013

⁴⁴ Gary McCormack, Rejish Nath, and Weibin Li, Dynamical excitation of maxon and roton modes in a Rydberg-dressed Bose-Einstein condensate, Phys. Rev. A 102, 023319 (2020) - Published 19 August 2020

⁴⁵ N. Henkel, R. Nath, and T. Pohl, Three-Dimensional Roton Excitations and Supersolid Formation in Rydberg-Excited Bose-Einstein Condensates, Phys. Rev. Lett. 104, 195302 (2010) - Published 11 May 2010

⁴⁶ Si-Cong Ji, Long Zhang, Xiao-Tian Xu, Zhan Wu, Youjin Deng, Shuai Chen, and Jian-Wei Pan, Softening of Roton and Phonon Modes in a Bose-Einstein Condensate with Spin-Orbit Coupling, Phys. Rev. Lett. 114, 105301 (2015) - Published 9 March 2015

⁴⁷ Hao Lyu, Yongping Zhang, and Thomas Busch, Detection of roton and phonon excitations in a spin-orbit-coupled Bose-Einstein condensate with a moving barrier, Phys. Rev. A 106, 013302 (2022) - Published 5 July 2022

⁴⁸ Jinwu Ye, Elementary excitations in a supersolid, Euro-physics Letters, 82 (2008) 16001

⁴⁹ Jinwu Ye, Elementary excitations, Spectral weights and Experimental signatures of a Supersolid and Larkin-Ovchinnikov-Fulde - Ferrell (LOFF) state, J. Low Temp Phys. 160(3), 71-111,(2010)

⁵⁰ In high temperature superconductors, the fermionic quasi-particle spectrum also acquires such an extra Doppler shift term due to the superflow of a vortex far away. See Jinwu Ye, Random magnetics fields and the quasi-particle transports in the mixed state of high T_c cuprates, Phys. Rev. Lett. 86, 316 (2001). Jinwu Ye, Thermally generated vortices, gauge invariance and electron spectral function in the pseudo-gap regime, Phys. Rev. Lett. 87, 227003 (2001).

⁵¹ Jinwu Ye, Random magnetics fields and the quasi-particle transports in the mixed state of high T_c cuprates, Phys. Rev. Lett. 86, 316 (2001).

⁵² Jinwu Ye, On Emery-Kivelson line and universality of Wilson ratio of spin anisotropic Kondo model, Phys. Rev. Lett. 77, 3224 (1996); Jinwu Ye, Abelian Bosonization approach to quantum impurity problems, Phys. Rev. Lett. 79, 1385 (1997)

⁵³ In quantum optics, one usually study atom-photon interaction in a frame rotating together with the external pumping frequency, such a frame is called rotating frame where the atom-photon interaction becomes time-independent. Unfortunately, so far, there is no work to study how to transfer the time-independent phenomena in the rotating frame back to the lab frame which is time-dependent.

⁵⁴ Jinwu Ye, Quantum Phases of Excitons and Their Detections in Electron-Hole Semiconductor Bilayer Systems, J. Low Temp Phys. 158(5), 882-900 (2010).

⁵⁵ To make a simple analogy here, a moving charge will produce a time-dependent EM field. but a line of moving charges form a steady current will produce a static magnetic field, so becomes time-independent.

⁵⁶ Lichen Chen and Jinwu Ye, preprint in preparation.